ACS OMEGA

http://pubs.acs.org/journal/acsodf

Article

Computational, Mechanistic, and Experimental Insights into Regioselective Catalytic C−C Bond Activation in Linear 1-Aza-[3]triphenylene

Jan Ulč, Yuya Asanuma, Robert Moss, Gabriele Manca,* Ivana Císařová, and Martin Kotora*

Cite This: *ACS Omega* 2022, 7, 8665−8674

Read Online

ACCESS | Metrics & More | Article Recommendations | Supporting Information

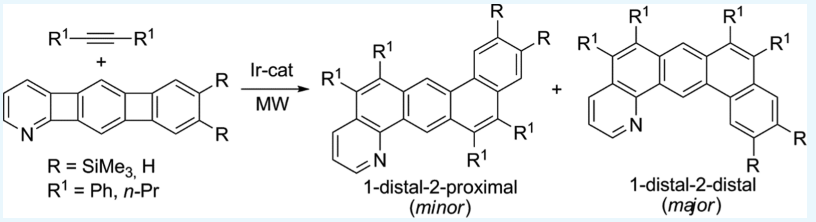

ABSTRACT: C−C bond activation by transition metal complexes in ring-strained compounds followed by annulation with unsaturated compounds is an efficient approach to generate structurally more complex compounds. However, the site of catalytic C−C bond activation is difficult to predict in unsymmetrically substituted polycyclic systems. Here, we report a study on the (regio)selective catalytic cleavage of selected C−C bonds in 1-aza-[3]triphenylene, followed by annulation with alkynes, forming products with extended π-conjugated frameworks. Based on density functional theory (DFT) calculations, we established the stability of possible transition metal intermediates formed by oxidative addition to the C−C bond and thus identified the likely site of C−C bond activation. The computationally predicted selectivity was confirmed by the following experimental tests for the corresponding Ir-catalyzed C−C cleavage reaction followed by an alkyne insertion that yielded mixtures of two mono-insertion products isolated with yields of 34−36%, due to the close reactivity of two bonds during the first C−C bond activation. Similar results were obtained for twofold Ir- or Rh-catalyzed insertion reactions, with higher yields of 72−77%. In a broader context, by combining DFT calculations, which provided insights into the relative reactivity of individual C−C bonds, with experimental results, our approach allows us to synthesize previously unknown pentacyclic azaaromatic compounds.

INTRODUCTION

The selective activation of unreactive C−C bonds is a key challenge in organic chemistry by opening up new and shorter synthetic paths to functionalized compounds such as natural products, various polyaromatic substances, and nanorings, among others.[1−8] Yet, this area remains mostly unexplored despite the abundance of potential targets and numerous possibilities for further development and expansion.

C−C bond activation studies should target substrates with several relatively equivalent cleavable bonds. However, cleavage may nevertheless occur at various sites, giving rise to mixtures of regioisomeric products. In such cases, computational modeling can theoretically explain the most likely reaction site by helping us to understand the reactivity of C−C bonds under specific experimental conditions and rationally designed reaction conditions. Therefore, theoretical modeling of the spatial arrangement and interaction energies of materials is crucial for a more detailed comprehension of molecular interactions between reactants and catalysts.[9−13]

In this respect, [n]phenylenes—compounds formed by alternating benzene and cyclobutadiene rings—can be envisioned as convenient candidates for C−C bond cleavage studies. Strain-relieve-driven catalytic activation of their C−C bonds yields species capable of participating in annulation reactions with unsaturated compounds and thus expands their molecular framework. Such **r**ing **e**xpansion/**a**nnulation (REAP) or cut-and-sew processes in smaller aromatic precursors stand out among the possible strategies for constructing polyaromatic hydrocarbons (PAHs) with extended planar π-conjugated systems considering the potential applications of these compounds in different fields of chemistry, e.g., materials science or organic electronics.[14,15]

These applications, however, require developing a new approach to synthesize specifically substituted products. The most well-known representatives of this class of compounds are biphenylenes and angular and linear [3]phenylenes. Biphenylenes have been used as substrates in numerous reports of a

Received: November 25, 2021
Accepted: February 18, 2022
Published: March 4, 2022

https://doi.org/10.1021/acsomega.1c06664
ACS Omega 2022, 7, 8665−8674

Scheme 1. Plausible Insertion Products: Four Regioisomeric Products Can Be Formed after the First C−C Activation and Insertion of an Alkyne Moiety into Aza[3]phenylenes

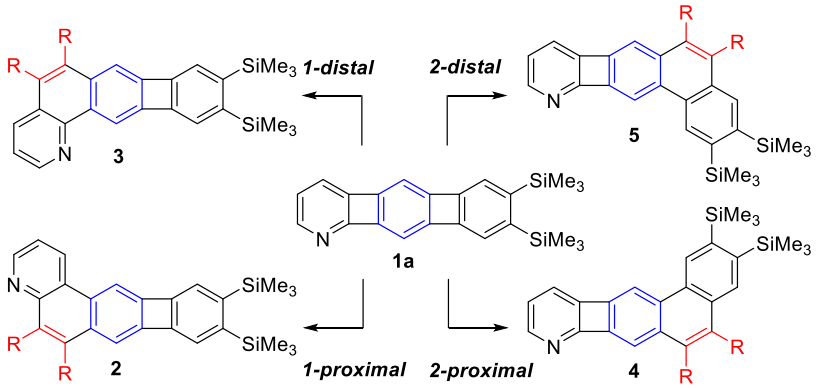

transition metal complex-catalyzed activation of the cyclobutadiene C−C bond followed by alkyne or nitrile insertion giving rise to 9,10-substituted phenanthrenes[16−18] or 9-substituted phenanthridines,[19] respectively. In turn, Ni-[20] or Ir-catalyzed[21] insertion to angular [3]phenylenes can give rise to picenes and other aromatics such as benzo[3,4]cyclobuta[1,2-*a*]phenanthrenes and benzo[*c*]chrysene, among others. In contrast, only one report has addressed a catalytic C−C bond activation in linear [3]phenylene (Ni-catalyzed alkyne insertion[22]), yielding a mixture of mono- and di-insertion products—benzo[3,4]cyclobuta[1,2-*b*]phenanthrene, benzo[*k*]tetraphene, and benzo[*m*]tetraphene. Similar insertions of their heteroaromatic analogues, which would lead to larger Ne-PAHs (*N*-embedded PAHs),[23−27] have surprisingly remained overlooked thus far.

In this context, we have recently reported a regioselective catalytic cleavage of proximal or distal C−C bonds in bistrimethylsilylated azabiphenylene.[28] The cleavage was followed by subsequent annulation with alkynes furnishing benzo[*f*]- and benzo[*h*] quinolines, depending on the catalytic conditions, and the presence of trimethylsilyl groups generally enhanced the C−C bond activation given the lower oxidative addition barrier to the C−C bond.[28] Our computational study helped us understand and rationalize the catalyst-dependent regioselective C−C cleavage. Based on our results, we explored the scope of selective C−C bond activation to bistrimethylsilylated 1-aza-[3]phenylene **1a**—a compound with a more intricate molecular architecture—for several fundamental and practical reasons. First, the X-ray diffraction data[29] of the parental 1-aza-[3]phenylene clearly showed that all four bonds connecting the aromatic rings are more or less of the same length (1.508−1.510 Å), thus making it difficult to identify the most reactive bond.[30] Second, assessing the relative bond reactivities in this molecule could provide information on regioselective C−C bond activation in even more complex molecules. Third, C−C bond activation and alkyne insertion could give access to tailored Ne-PAHs with specific architectures. Bistrimethylsilyl 1-aza-[3]phenylene **1a** has four nonequivalent C−C bonds, unlike bistrimethylsilylated azabiphenylene, which contains two nonequivalent bonds. As such, four different regioisomers could be formed upon the first C−C bond activation followed by mono-insertion of an alkyne (Scheme 1).

Considering the above, we hypothesized that one-pot selective insertion(s) of alkynes in azaaromatic compounds bearing two cyclobutadiene rings could open a short pathway to new specifically polysubstituted azaaromatic compounds with complex architectures that would otherwise be difficult to prepare. In addition, these compounds could be candidates for new applications in materials science because they are regioisomeric to structurally related compounds such as dibenzoacridine.[31−33] To test our hypothesis, we aimed (i) to establish the order of the C−C bond cleaved and (ii) to assess whether one-pot multiple insertions can lead to compounds with five aromatic rings. More specifically, using a combined computational and experimental approach, we studied the selective C−C bond activation in bistrimethylsilylated 1-aza-[3]phenylene **1a**. Following our theoretical findings, we experimentally verified the reactivity of each C−C bond, thereby devising a rapid and modular strategy for selective twofold C−C bond activation followed by alkyne insertion, forming Ne-PAHs with extended π-systems. The experimental results matched with the computational ones.

RESULTS AND DISCUSSION

DFT Calculations. At the outset, theoretical calculations were made to shed light on a possible course of the reaction (for details see the Supporting Information). The first step of the analysis was to establish the most stable isomer of the insertion reaction between substrate **1a** and the alkyne catalyzed by the Ir complex. Although we did not identify any substantial energy variation, our calculations revealed that the two most probable activation sites are the C−C bonds near the Si-substituted ring in **4** and **5**, with a quasi-negligible stabilization in favor of the 2-distal C−C bond in **5** (Table 1).

Table 1. Relative Free Energy (kcal·mol^{-1}) for the Four Different Isomers Calculated at Two Different Temperatures, 298.15 and 443.0 K, Respectively

isomer	compound	relative free energy (kcal·mol^{-1}, 298.15 K)	relative free energy (kcal·mol^{-1}, 443.0 K)
1-proximal	**2**	+3.3	+3.6
1-distal	**3**	+0.9	+1.4
2-proximal	**4**	+0.09	+0.13
2-distal	**5**	0	0

Since the first screening did not provide any useful information on selectivity, we focused on the most favorable C−C bond cleavage in the cyclobutadiene rings of the substrate. The most probable process of catalyst activation is the dissociation of the dinuclear precursor [IrCl(COD)]$_2$, which, in the presence of dppe, allows the formation of two

https://doi.org/10.1021/acsomega.1c06664
ACS Omega 2022, 7, 8665−8674

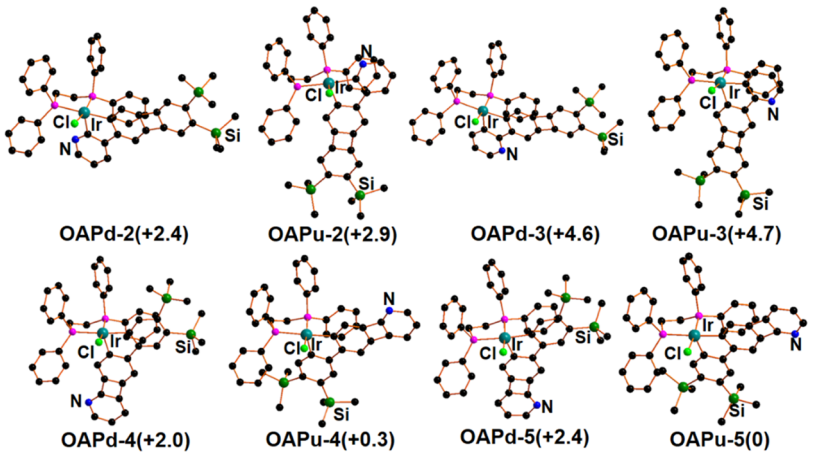

Figure 1. Optimized structures of the eight different isomers with the relative free energy (in parenthesis in kcal·mol^{-1}). The hydrogen atoms were hidden for clarity.

coordinatively unsaturated trigonal planar IrCl(dppe) units releasing two COD molecules (for details, see the Supporting Information). This IrCl(dppe) unit is thus ready to interact with one of the four C−C bonds in the four-membered rings to promote the formation of the oxidative addition product.

In the first step of our computational analysis, we optimized the adducts of the IrCl(dppe) unit with the pyridine nitrogen atom and with the double bonds of the skeleton of **1a** as a potential starting point. The formation of the adduct between the coordinative unsaturated fragment IrCl(dppe) and the substrate, namely, **Nadd-1**, through the pyridine nitrogen has been estimated to be particularly exergonic by −22.3 kcal·mol^{-1}, shown in Figure S1. On the contrary, the formation of any adduct between the metal fragment and one of the C═C bonds of the substrate has been estimated to be slightly exergonic by 1−3 kcal·mol^{-1}; thus, the temperature should be fundamental for overcoming the energy differences and promoting in some way the development of the reaction. In the second step, we analyzed all possible isomers of the oxidative addition intermediates—oxidative addition products (OAP)—provided by the interaction between the unsaturated IrCl(dppe) fragment and one C−C bond of the cyclobutadiene rings. Figure 1 reported all of the eight optimized compounds (two isomers for each product, depending on the N position above or under the coordination plane) together with their relative free energy (in kcal·mol^{-1}) considering the most stable structure of the 5-dist-up isomer OAPu-**5** as the zero-energy point.

Although the complex (OAPu-**5**) is only slightly favored at room temperature, the free energy differences are too small to prefer one to the other. In this view, we optimized all of the possible transition states, one for each of the eight isomers shown in Figure 1, and we found that the transition states for the isomers 2-prox-up (OAPu-**4**) and 2-dist-up (OAPu-**5**) are at lower energy than the other ones involving the two C−C linkages more proximal to the nitrogen center. In particular, the calculations highlight a free energy limiting difference between the **TSu-5** or **TSu-4** and the **TSd-2** of ca. 12 kcal·mol^{-1}. The three previously mentioned transition states are reported in Figure 2 while all of the other five are shown in the Supporting Information, Figure S2.

The free energy pathways for the three different isomers of the oxidative addition process are shown in Figure 3 together with the associated free energy costs and gains. The first adduct is particularly favored for its anchorage to the pyridinic nitrogen

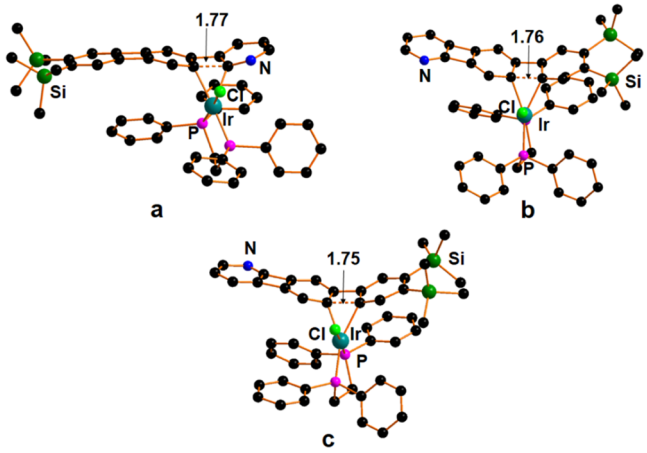

Figure 2. Optimized structures for the transition state: (a) 1-prox-down (TSd-2), (b) 2-dist-up (TSu-4), and (c) 2-prox-up (TSu-5), respectively.

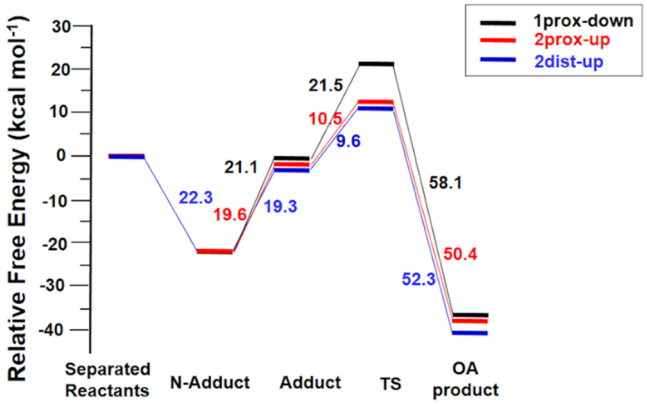

Figure 3. Free energy (kcal·mol^{-1}) profile of the evolution from the separated reactants up to the transition state and to the final oxidative addition (OA) products. Black: **TSd-2** and **OAd-2**; red: **TSu-4** and **OAu-4**; and blue: **TSu-5** and **OAu-5**.

over any other interaction between the unsaturated Ir(dppe)Cl and any unsaturated bond of the substrate. After the cleavage of the Ir−N bonding, the system reasonably evolves toward the coordination of a C−C bonding, followed by its cleavage. The free energy barriers associated with the breaking of the 2-dist-up

https://doi.org/10.1021/acsomega.1c06664
ACS Omega 2022, 7, 8665−8674

Table 2. Catalytic Insertion Reaction of Diphenylethyne and 4-Octyne with 1a

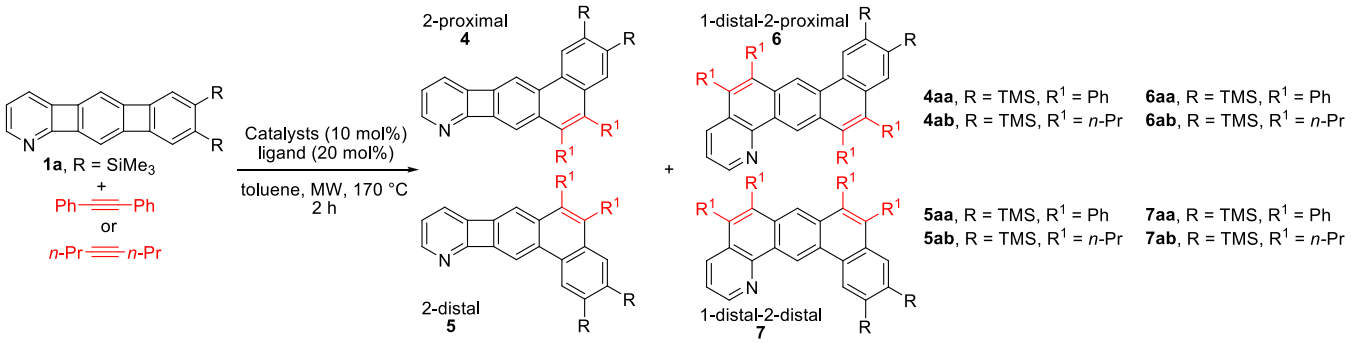

					yields[a,bc]					
entry	catalyst	ligand	R^1	(equiv)	**4aa** (%)	**5aa** (%)	C.Y. (%)[b]	**6aa** (%)	**7aa** (%)	C.Y. (%)[b]
1[d]	$[Ir(cod)Cl]_2$	dppe	Ph	2	<3	<3		0	0	
2		dppe	Ph	1	8	24	32	0	0	
3		dppe	Ph	2	0	0		25	45	70
4		dppe	Ph	10	0	0		22	50	72
5		dppp	Ph	2	8	12	20	4	22	26
6		dppp	Ph	10	10	10	20	8	17	25
7	$[Rh(cod)Cl]_2$	dppe	Ph	2	0	0		17	33	50
8		dppe	Ph	10	0	0		26	46	72
9		dppp	Ph	2	<3	<3		<3	<3	
10[e]	$[Rh(cod)_2]BF_4$	dppe[f]	Ph	10	15	21	36	<3	<3	
					4ab (%)	**5ab** (%)		**6ab** (%)	**7ab** (%)	
11	$[Ir(cod)Cl]_2$	dppe	*n*-Pr	1	14	20	34	0	0	
12		dppe	*n*-Pr	10	0	0		26	51	77

[a]Isolated yields. [b]Combined yields. [c]<3% denotes the amount of the product that was detected by TLC but could not be isolated in sufficient purity. [d]Oil bath. [e]THF instead of toluene. [f]10 mol %.

(**TSu-5**) C−C bond (+9.6 kcal·mol^{-1}) are lower than that of the first adduct, followed by the free energy barrier of 2-dist-down (**TSu-4**) (+11.5 kcal·mol^{-1}). The highest value is associated with the 1-prox-down (**TSd-2**) isomer (+21.5 kcal·mol^{-1}) and thus clearly indicating that 2-dist and 2-prox bonds are preferentially cleaved. The difference of 0.9 kcal·mol^{-1} between **TSu-4** and **TSu-5** indicates that they should be formed in a ∼3:1 ratio. This result agrees with the calculated Wiberg index bond order, which predicted the lowest bond order for the 2-dist and 2-prox positions in the starting adducts.

In summary, our DFT calculations showed that the first cleavage should occur at distal C−C bonds, with a slight preference for the 2-distal C−C bond, followed by the cleavage of the 2-proximal C−C bond.

Insertion Reactions. The starting 7,8-bis(trimethylsilyl)1-azatriphenylene **1a** was prepared according to the procedure described by Vollhardt et al.,[29] with small modifications from 5,6-bis(trimethylsilyl)-1-azabiphenylene, in an overall yield of 40%. Its nonsilylated analogue **1b** was prepared by desilylation of **1a** with CF_3COOH in dichloromethane in 89% yield. For synthesis details, see the Supporting Information.

Our preliminary calculations on the catalytic action of Ir/dppe indicated that the most vulnerable bonds in **1a** should be the 2-proximal and 2-distal bonds, where C−C bond activation likely occurs, giving rise, after a reaction with an alkyne, to the respective insertion products **4** (5,6-diR'-2,3-diRphenanthro-[3',2':3,4]cyclobuta[1,2-*b*]pyridines) and **5** (5,6-diR'-2,3-diRphenanthro[2',3':3,4]cyclobuta[1,2-*b*]pyridines). With this knowledge, we studied insertion reactions with diphenylethyne (Table 2). At the outset, we performed the insertion of diphenylethyne into **1a** under the previously used conditions using an Ir/dppe catalytic system[21] at 130 °C (entry 1). However, only traces of products **4aa** and **5aa** were formed. By contrast, when MW heating (170 °C) was applied, we observed a rapid C−C bond cleavage followed by insertion of diphenylethyne providing products **4aa** and **5aa** in promising isolated yields of 8 and 24% (32% overall yield), respectively (entry 2). The 1:3 ratio of **4aa** (the product of the 2-proximal C−C bond cleavage) and **5aa** (the product of the 2-distal C−C bond cleavage) is in agreement with the prediction based on the DFT calculation. Along with these two major products, other minor aromatic side-products were detected as well, judging from our TLC analysis. However, isolation did not provide them in sufficient amounts for full and unequivocal characterization. In turn, we did not detect traces of di-insertion products of the second C−C bond cleavage followed by diphenylethyne insertion. The combination between experimental and computational results suggested that also in the case of Ir in place of Rh the sites of preferential C−C bond activation should be the same.

After developing this approach for selective mono-insertion, we then tried to increase the yields of the mono-insertion product and also to induce the second C−C bond cleavage to achieve a twofold insertion. For this purpose, we performed the reactions with 2 and 10 equiv of the alkyne with respect to **1a** (entries 3 and 4). Workup of the reaction mixtures in both instances provided only mixtures of the double-insertion products **6aa** and **7aa** in isolated yields of 25 and 22, and 45 and 50%, respectively (70 and 72% overall yield, respectively). Traces of monoinsertion products were not detected. Gratifyingly, compounds **6aa** and **7aa** were readily separable by simple column chromatography. In short, the predominant (sole)

https://doi.org/10.1021/acsomega.1c06664
ACS Omega 2022, 7, 8665−8674

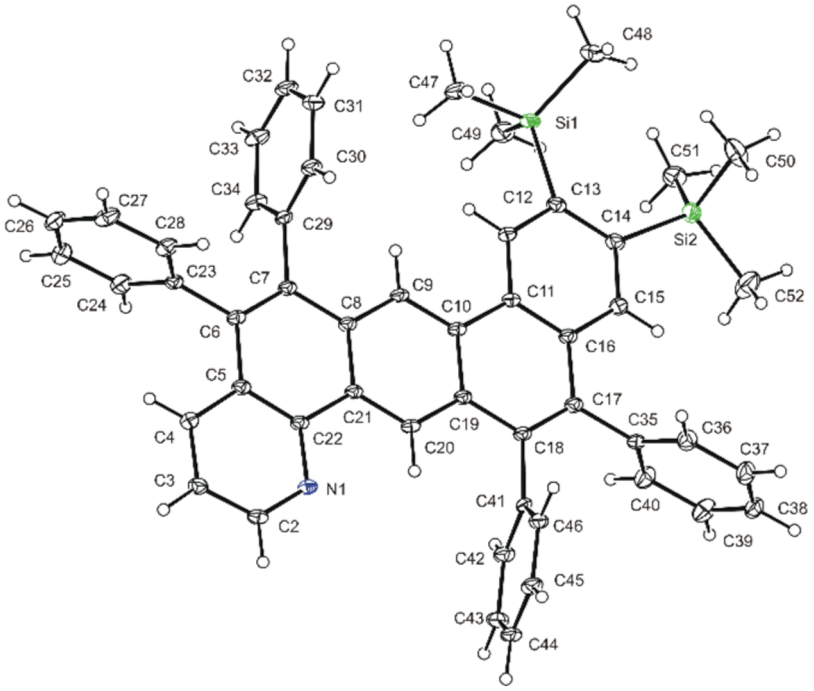

Figure 4. ORTEP plot of **6aa**. Ellipsoids are shown at 50% probability.

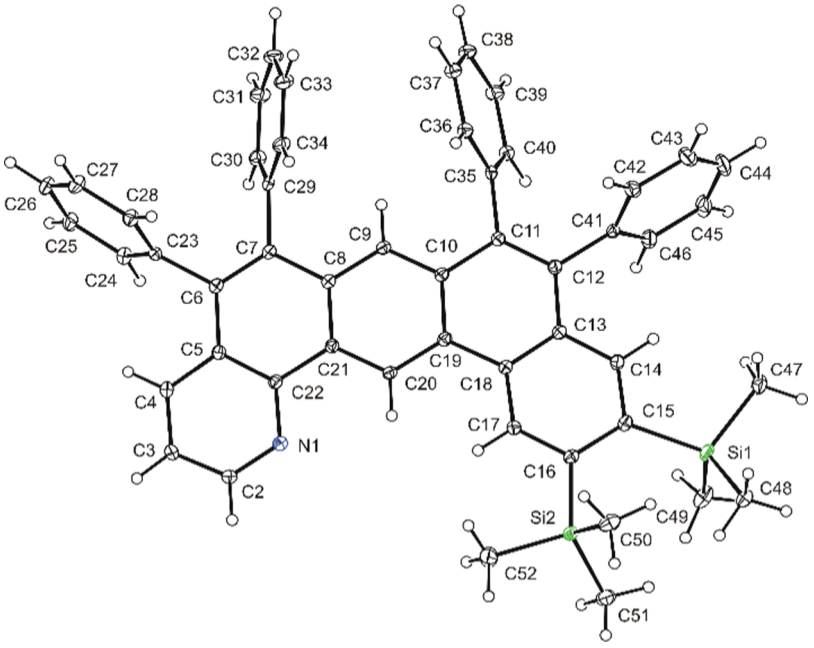

Figure 5. ORTEP plot of **7aa**. Ellipsoids are shown at 50% probability.

formation of the double-insertion products indicates that the 1-distal C−C bond in the mono-insertion products **4** and **5** is relatively readily activated in comparison with the cleavage of C−C bonds in **1a**, confirming the DFT results. As far as the regioselective aspect is concerned, the preferential activation of the 1-distal C−C bond is in line with previous observations obtained from studies of alkyne insertion to 1-azabiphenylene. Next, we decided to change the Ir/dppe catalytic system for the Ir/dppp one because it gave better results for the distal C−C bond activation in azabiphenylene.[28] However, its use in a reaction of **1a** with diphenylethyne provided a mixture of mono- and di-insertion products **4aa**−**7aa** regardless of 2- or a 10-fold excess of diphenylethyne (entries 5 and 6). Workups of the respective reaction mixture enabled us to isolate the mono-insertion products **4aa** and **5aa** in 8 and 12% and in 10 and 10% yields and the di-insertion products **6aa** (7,8,12,13-tetraRphenathro[3,2-*h*]quinolines) and **7aa** (5,6,8,9-tetraRphenanthro[2,3-*h*]quinolines) in 4 and 22% and in 8 and 17% yields, respectively. The structures of **6aa** and **7aa** were unequivocally confirmed by single-crystal X-ray analyses (Figures 4 and 5).

To assess the catalytic activity of other group IX transition metal-based catalysts, we tested the Rh/dppe catalytic system. The reactions were run with 2 and 10 equiv of diphenylethyne,

https://doi.org/10.1021/acsomega.1c06664
ACS Omega 2022, 7, 8665−8674

obtaining mixtures of double-insertion products **6aa** and **7aa** in both cases (entries 7 and 8). The former yielded **6aa** and **7aa** in 17 and 33% (50% overall yield) and the latter in 26 and 46% (72% overall yield), respectively. The mono-insertion products were not detected in the respective reaction mixtures, thus confirming that the 1-distal C−C bond in **4** or **5** can be more easily activated than the 1-proximal bond. This result seems to be in line with the obtained computational findings of a very low barrier associated with the second insertion process compared to the first one, providing a reasonable justification for the missing detection of mono-insertion products.

Surprisingly, the Rh/dppp system did not lead to products (entry 9). We also tested a cationic Rh-based system ($[Rh(cod)_2]BF_4$) (entry 10), and it showed high selectivity for the mono-insertion products but low catalytic activity. Products **4aa** and **5aa** were isolated in only 15 and 21% yields (36% overall yield), respectively, despite the large excess of diphenylethyne (10 equiv). Di-insertion products **6aa** and **7aa** were detected in trace amounts only. The reaction of **1a** was also performed with 1 or 10 equiv of 4-octyne under standard conditions (entries 11 and 12). The former case gave rise to a mixture of mono-insertion products **4ab** and **5ab** in 14 and 20% yields (34% combined yield). Di-insertion products were not detected. The latter one exclusively yielded a mixture of **6ab** and **7ab** in 26 and 51% yields (77% combined yield). The mono-insertion products **4ab** and **5ab** were detected only in trace amounts.

Desilylation under acidic conditions of the maternal silylated compounds **6aa**, **6ab**, **7aa**, and **6ab** provided **10a** (65%), **11a** (59%), **10b** (76%), and **11b** (88%), respectively (Scheme 2).

Scheme 2. Desilylation of 6 and 7 to 10 and 11, Respectively

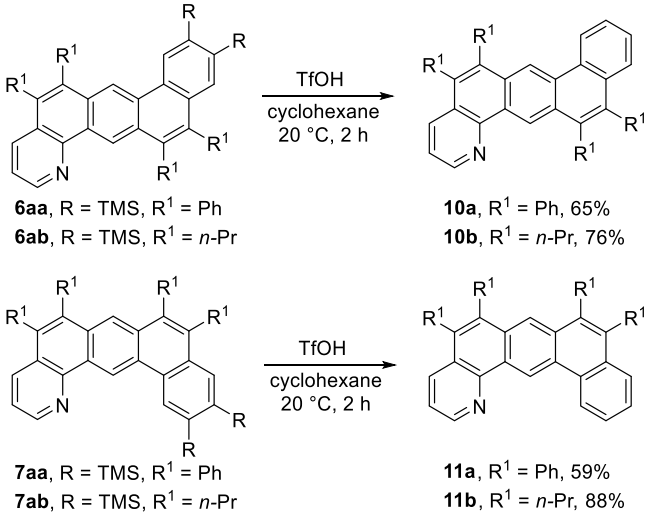

Finally, the reaction of 1-aza-[3]phenylene **1b** (**1a** without the $SiMe_3$ groups) with diphenylethyne, under the conditions described in entry 4 (Table 2), provided a mixture of di-insertion products **10a** and **11a** in 19 and 40% yields (59% overall yield), respectively (Scheme 3). The mono-insertion products **8a** and **9a** were detected only in trace amounts.

Since compounds **11a** and **11b** were obtained in larger amounts by desilylation of **7aa** and **7ab**, we attempted annulations of **11a** and **11b** with diphenylethyne and 4-octyne to obtain the respective quinolizinium salts using various catalytic systems (Table 3, for a full account, see Table S1 in the

Scheme 3. Insertion of Diphenylethyne into 1b

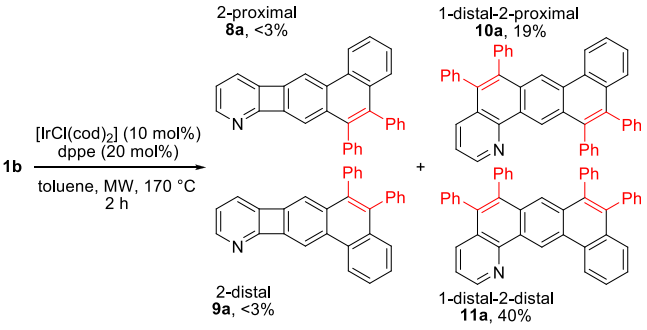

Supporting Information). At the outset, the standard conditions ($[Cp^*RhCl_2]_2$, $Cu(BF_4)_2$, O_2, 50 °C)[34] were applied, but the reaction did not proceed. Replacing the Rh catalyst with Co or Ir catalysts did not yield the expected products either. Ultimately, we tested systems combining $Cu(OAc)_2$ with $AgBF_4$ as an oxidant at 100 °C for the annulations of **11a** and **11b** with diphenylethyne and 4-octyne, thereby obtaining the expected products **12a** and **12b** in 53 and 59% yields, respectively (entries 1 and 2). Co- or Ir-based catalysts fared poorly; the former did not provide any product, and the latter gave **12b** in a meager 9% yield (entries 3 and 4). Single-crystal X-ray diffraction analysis of **12a** unequivocally confirmed its structure (Figure 6). Thanks to its higher reactivity, the Rh catalyst was more successful than the Ir catalyst.[35,36]

Subsequent attempts to conduct the reactions of **10a** and **10b** with diphenylethyne or 4-octyne under the previously mentioned conditions and switching to various catalysts and different reaction temperatures were unsuccessful. Only after changing to the cationic Rh-complex ($[Rh(cod)_2]BF_4$), the reactions of **10a** and **10b** with diphenylethyne and 4-octyne yielded the desired products **13a** and **13b**, albeit in low isolated yields of ∼5% (Scheme 4). We presume that the lower ability of **10a** and **10b** to undergo annulation with alkynes is caused by steric hindrance exerted by the phenyl and *n*-Pr groups in position 13 that shield the C−H bond in position 14. This steric hindrance is evident in the X-ray structure of **10b** (Figure 4).

X-ray Crystal Structures. Single crystals of **6aa**, **7aa**, and **11aa** were grown by hexane diffusion into their CH_2Cl_2 solutions, solving the crystal structures by single-crystal X-ray diffraction analysis (Figures 4−6). The crystal structure of **6aa** revealed that the phenanthro[3,2-*h*]quinoline scaffold is almost planar, as expected. The dihedral angle values for ∠N1-C22-C21-C20 and ∠C9-C10-C11-C12 of the bay regions[37] are only 1.7 and 2.0°, respectively. The latter lies within the interval of dihedral angle values typical of structurally related compounds with the benzo[*k*]tetraphene scaffold, which range from 0.0 to 5.9°, depending on the respective substitution pattern.[38−41]

The crystal structure of **7aa** revealed that the phenanthro[2,3-*h*]quinoline scaffold adopts a slightly helical arrangement, as shown by two dihedral angles of two neighboring bay regions: ∠N1-C22-C21-C20 is 1.7° and ∠C20-C19-C18-C17 is 12.9°. The distance between H20 and H17 is 2.12 Å. The sum of the angles is two times lower than that of the structurally related compound with the benzo[*m*]tetraphene scaffold (20.4 and 25.8°).[42]

The molecule **12a** partly assumes a helical shape due to its [4]helicene arrangement. The naphthoquinolizinium fragment in **12a** is almost planar, with dihedral angles ∠N1-C22-C21-C8 179.1° and ∠N1-C22-C21-C20 of 1.3°, resulting from ring

https://doi.org/10.1021/acsomega.1c06664
ACS Omega 2022, 7, 8665−8674

Table 3. C−H Activation-Based Annulations of 11 with Diphenylethyne and 4-Octyne to 12

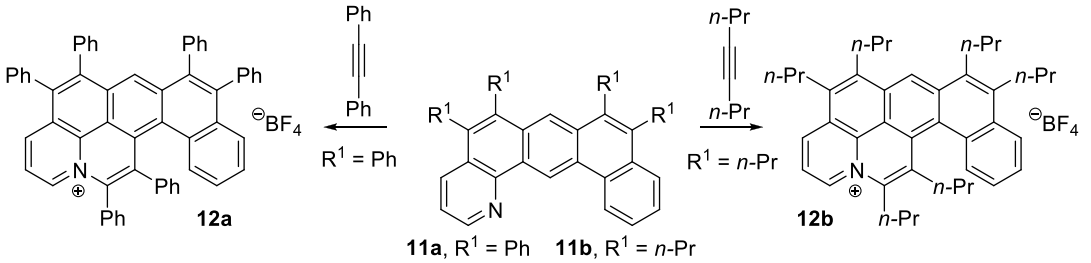

Catalyst (10 mol%), $Cu(OAc)_2$ (20 mol%), $AgBF_4$ (1 eq), DCE, 100 °C.

entry	compound	catalyst	alkyne	12	isolated yields (%)
1	**11a**	$[Cp^*RhCl_2]_2$	Ph	**12a**	53
2	**11b**	$[Cp^*RhCl_2]_2$	*n*-Pr	**12b**	59
3	**11b**	Cp^*CoI_2	*n*-Pr	**12b**	0
4	**11b**	$[Cp^*IrCl_2]_2$	*n*-Pr	**12b**	9

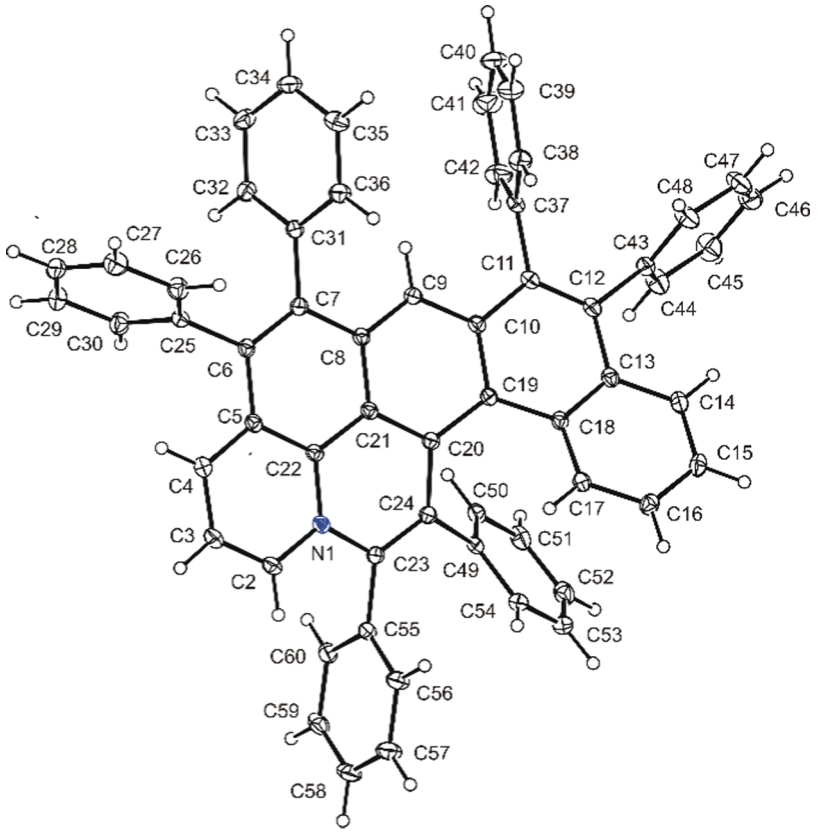

Figure 6. ORTEP plot of **12a**. Ellipsoids are shown at 50% probability.

Scheme 4. C−H Activation-Based Annulations of 10

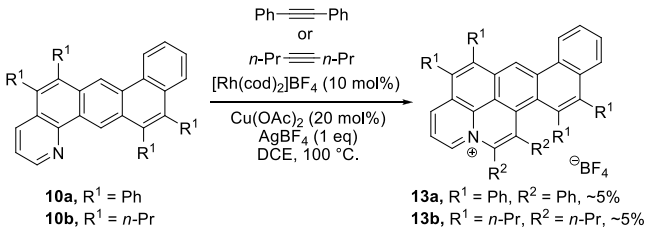

10a, R^1 = Ph
10b, R^1 = *n*-Pr

13a, R^1 = Ph, R^2 = Ph, ~5%
13b, R^1 = *n*-Pr, R^2 = *n*-Pr, ~5%

fusion. Four aromatic rings on the right-hand side form the [4]helicene arrangement with dihedral angles ∠C24-C20-C18-C18 and ∠C20-C19-C18-C17 of 27.1 and 23.4°, totaling 50.5°. The sum of the dihedral angles is similar to that of 1-Ph[4]helicene, which is ~48°.[43] Conjugation between the naphthoquinolizinium moiety and the [4]helicene backbone can nevertheless occur and affect its optoelectronic properties. As for the phenyl substituents, their orientation is unsurprisingly almost perpendicular to the basic framework.

Photochemical Properties. Figure 7 shows the UV/Vis absorption and fluorescence spectra of **12a** and **12b** in dichloromethane, and the spectral data are summarized in Table S3. The spectra differ only slightly, showing characteristic absorption bands around 380, 458, and 488 nm (for **12a**) and 373, 459, and 489 nm (for **12b**). The photoluminescence (PL) properties of **12a** and **12b** were also examined in dichloro-

https://doi.org/10.1021/acsomega.1c06664
ACS Omega 2022, 7, 8665−8674

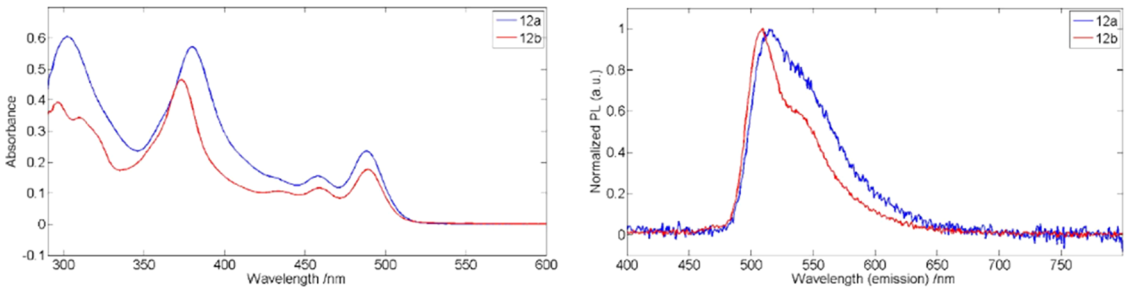

Figure 7. Absorption and emission spectra. Absorption (left) and normalized emission (right) spectra of **12a** (blue) and **12b** (red) were recorded as CH_2Cl_2 solutions.

methane solutions at room temperature. Both compounds behave as fluorescent emitters, and the fluorescence spectra are unresolved with maxima at λ_{em} = 516 (**12a**) and 506 (**12b**) nm (Figure 7). These values are red-shifted by ∼40 and 50 nm in comparison with their maternal 5,6,10,11-tetraphenyl (λ_{em} = 477 nm) and 5,6-dipropyl-10,11-diphenyl (λ_{em} = 457 nm) naphtho[2,1,8-*ija*]quinolizinium salts, which also had unresolved emission spectra.[44] The emission quantum yields (Φ) were Φ_{abs} = 0.46 (**12a**) and 0.45 (**12b**).

In summary, the combined computational/experimental approaches allow a (regio)selective activation of C−C bonds in substrates with several similar reactive sites. Our results clearly show that a one-pot C−C activation/alkyne insertion reaction sequence is a feasible strategy for transforming strained aromatic molecules (linear aza[3]phenylene) into larger and specifically substituted π-conjugated *N*-embedded aromatic systems.

First, our DFT calculations, based on thermodynamic analysis, highlighted the preferential sites of C−C activation in the framework of linear 1-aza[3]phenylene. Second, our experiments confirmed all DFT results, according to which two regioisomeric mono-insertion products are formed. Third, the major reaction pathway is a twofold insertion in the presence of excess of an alkyne, giving rise to products with the phenathro[3,2-*h*]quinolines (**6**) and phenathro[2,3-*h*]quinoline (**7**) frameworks in high yields and selectivity. Finally, our preliminary experiments have shown that **9** can undergo C−H bond activation-triggered annulation, yielding quinolizinium salts. These findings demonstrate that DFT calculations can be used to provide useful hints on a synthetic route based on the ring-opening of azapolyphenylenes as a straightforward access to previously unknown, region-defined, fully aromatic azaPAHs with potential applications in organic electronics. Thus, such a ring expansion/annulation process (REAP) offers a complementary strategy to recently reported procedures, such as aza-APEX based on the reaction of an in situ generated nitrilium cation with aromatic compounds,[45] rhoda-electrocatalyzed domino alkyne annulations[46] or the π-extension of heteroaryl halides[47] because these methods cannot be used in our starting materials.

■ ASSOCIATED CONTENT

Supporting Information

The Supporting Information is available free of charge at https://pubs.acs.org/doi/10.1021/acsomega.1c06664.

Experimental procedures; DFT calculations; X-ray data; and copies of spectra, among other materials and are available online; 21-Ulc-D-SI-Experimental (PDF)

6aa-cu_ju_rm1_kotora (CIF)

7aa-cu_ju_rm2_kotora_sq (CIF)

12a-cu_ju_834_p_b_kotora (CIF)

■ AUTHOR INFORMATION

Corresponding Authors

Gabriele Manca − *CNR-ICCOM, 50019 Sesto Fiorentino Firenze, Italy;* orcid.org/0000-0003-2068-1731; Email: gmanca@iccom.cnr.it

Martin Kotora − *Department of Organic Chemistry, Charles University, Prague 12800, Czech Republic;* orcid.org/0000-0003-4491-7091; Email: kotora@natur.cuni.czulč

Authors

Jan Ulč − *Department of Organic Chemistry, Charles University, Prague 12800, Czech Republic*

Yuya Asanuma − *Department of Organic Chemistry, Charles University, Prague 12800, Czech Republic*

Robert Moss − *Department of Organic Chemistry, Charles University, Prague 12800, Czech Republic;* Present Address: LGC Link, 3 Mallard Way, Strathclyde Business Park, Bellshill, Lanarkshire ML4 3BF, Scotland

Ivana Císařová − *Department of Inorganic Chemistry, Charles University, Prague 12800, Czech Republic; CNR-ICCOM, 50019 Sesto Fiorentino Firenze, Italy*

Complete contact information is available at: https://pubs.acs.org/10.1021/acsomega.1c06664

Author Contributions

The manuscript was written through contributions of all authors. All authors have given approval to the final version of the manuscript.

Notes

The authors declare no competing financial interest.

■ ACKNOWLEDGMENTS

M.K. gratefully acknowledges the financial support from the Czech Science Foundation (grant no. 21-12924S) and the Charles University Grant Agency (grant no. 1190218).

■ REFERENCES

(1) Souillart, L.; Cramer, N. Catalytic C−C Bond Activations via Oxidative Addition to Transition Metals. *Chem. Rev.* **2015**, *115*, 9410−9464.

(2) Murakami, M.; Ishida, N. Potential of Metal-Catalyzed C−C Single Bond Cleavage for Organic Synthesis. *J. Am. Chem. Soc.* **2016**, *138*, 13759−13769.

(3) Kondo, T. Ruthenium- and Rhodium-Catalyzed Strain-Driven Cleavage and Reconstruction of the C−C Bond. *Eur. J. Org. Chem.* **2016**, *2016*, 1232−1242.

(4) Chen, P.-H.; Billett, B. A.; Tsukamoto, T.; Dong, G. "Cut and Sew" Transformations via Transition-Metal-Catalyzed Carbon−Carbon Bond Activation. *ACS Catal.* **2017**, *7*, 1340−1360.
(5) Fumagalli, G.; Stanton, S.; Bower, J. F. Recent Methodologies That Exploit C−C Single-Bond Cleavage of Strained Ring Systems by Transition Metal Complexes. *Chem. Rev.* **2017**, *117*, 9404−9432.
(6) Song, F.; Gou, T.; Wang, B.-Q.; Shi, Z.-J. Catalytic activations of unstrained C−C bond. involving organometallic intermediates. *Chem. Soc. Rev.* **2018**, *47*, 7078−7115.
(7) Wang, B.; Perea, M.; Sarpong, A.; Transition Metal-Mediated, R.; Single Bond, C−C. Cleavage: Making the Cut in Total Synthesis. *Angew. Chem., Int. Ed.* **2020**, *59*, 18898−18919.
(8) Murakami, M.; Ishida, N. Cleavage of Carbon−Carbon σ-Bonds of Four-Membered Rings. *Chem. Rev.* **2021**, *121*, 264−299.
(9) For example, C-C bond cleavage in unsymmetrically substituted cyclopentanones Xiao, D.; Zhao, L.; Andrada, D. (**2019**). DFT Study of Unstrained Ketone C-C Bond Activation via Rhodium(I)-Catalyzed Suzuki-Miyaura Cross-Coupling Reactions. *ChemRxiv. Preprint.* DOI: 10.26434/chemrxiv.11288573.v1.
(10) Politano, F.; Sandoval, A. L.; Uranga, J. G.; Buján, E. I.; Leadbeater, N. E. Using experimental and computational approaches to probe an unusual carbon−carbon bond cleavage observed in the synthesis of benzimidazole N-oxides. *Org. Biomol. Chem.* **2021**, *19*, 208−215.
(11) Wang, M.; Li, M.; Yang, S.; Xue, X.-S.; Wu, X.; Zhu, C. Radical-mediated C-C cleavage of unstrained cycloketones and DFT study for unusual regioselectivity. *Nat. Commun.* **2020**, *11*, No. 672.
(12) Kosar, N.; Ayub, K.; Gilani, M. A.; Mahmood, T. Benchmark DFT studies on C−CN homolytic cleavage and screening the substitution effect on bond dissociation energy. *J. Mol. Model.* **2019**, *25*, No. 47.
(13) Xu, J.; Cui, Z.; Nie, K.; Cao, H.; Jiang, M.; Xu, H.; Tan, T.; Liu, L. A Quantum Mechanism Study of the C-C Bond Cleavage to Predict the Bio-Catalytic Polyethylene Degradation. *Front. Microbiol.* **2019**, *10*, No. 489.
(14) Zhang, L.; Cao, Y.; Colella, N. S.; Liang, Y.; Bredas, J.-L.; Houk, K. N.; Briseno, A. L. Unconventional, Chemically Stable, and Soluble Two-Dimensional Angular Polycyclic Aromatic Hydrocarbons: From Molecular Design to Device Applications. *Acc. Chem. Res.* **2015**, *48*, 500−509.
(15) Aumaitre, C.; Morin, J.-F. Polycyclic Aromatic Hydrocarbons as Potential Building Blocks for Organic Solar Cells. *Chem. Rec.* **2019**, *19*, 1142−1154.
(16) Perthuisot, C.; Edelbach, B. L.; Zubris, D. L.; Simhai, N.; Iverson, C. N.; Müller, C.; Satoh, T.; Jones, W. D. Cleavage of the carbon−carbon bond in biphenylene using transition metals. *J. Mol. Catal. A: Chem.* **2002**, *189*, 157−168.
(17) Steffen, A.; Ward, R. M.; Jones, W. D.; Marder, T. B. Dibenzometallacyclopentadienes, boroles and selected transition metal and main group heterocyclopentadienes: Synthesis, catalytic and optical properties. *Coord. Chem. Rev.* **2010**, *254*, 1950−1976.
(18) Takano, H.; Ito, T.; Kanyiva, K. S.; Shibata, T. Recent Advances of Biphenylene: Synthesis, Reactions and Uses. *Eur. J. Org. Chem.* **2019**, *2019*, 2871−2883.
(19) Korotvička, A.; Frejka, D.; Hampejsová, Z.; Císařová, I.; Kotora, M. Synthesis of Phenanthridines via a Rhodium-Catalyzed C−C Bond Cleavage Reaction of Biphenylene with Nitriles. *Synthesis* **2016**, *48*, 987−996.
(20) Gu, Z.; Boursalian, G. B.; Gandon, V.; Padilla, R.; Shen, H.; Timofeeva, T. V.; Tongwa, P.; Vollhardt, K. P. C.; Yakovenko, A. A. Activated Phenacenes from Phenylenes by Nickel-Catalyzed Alkyne Cycloadditions. *Angew. Chem., Int. Ed.* **2011**, *50*, 9413−9417.
(21) Korotvička, A.; Císařová, I.; Roithová, J.; Kotora, M. Synthesis of Aromatic Compounds by Catalytic C−C Bond Activation of Biphenylene or Angular [3]Phenylene. *Chem. - Eur. J.* **2012**, *18*, 4200−4207.
(22) Gu, Z.; Vollhardt, K. P. C. Phenylated Benzotetraphenes (Dibenzanthracenes) by Nickel-Catalyzed Diphenylacetylene Cycloadditions to Linear [3]Phenylenes. *Synthesis* **2013**, *45*, 2469−2473.
(23) Bunz, U. H. F. The larger N-heteroacenes. *Pure Appl. Chem.* **2010**, *82*, 953−968.
(24) Gu, P.-Y.; Wang, Z.; Zhang, Q. Azaacenes as active elements for sensing and bio applications. *J. Mater. Chem. B* **2016**, *4*, 7060−7074.
(25) Bunz, U. H. F.; Freudenberg, J. N-Heteroacenes and N-Heteroarenes as N-Nanocarbon Segments. *Acc. Chem. Res.* **2019**, *52*, 1575−1587.
(26) Müller, M.; Ahrens, L.; Brosius, V.; Freudenberg, J.; Bunz, U. H. F. Unusual stabilization of larger acenes and heteroacenes. *J. Mater. Chem. C* **2019**, *7*, 14011−14034.
(27) Zhang, Z.; Zhang, Q. Recent progress in well-defined higher azaacenes (n ≥ 6): synthesis, molecular packing, and applications. *Mater. Chem. Front.* **2020**, *4*, 3419−3432.
(28) Frejka, D.; Ulč, J.; Kantchev, E. A. B.; Císařová, I.; Kotora, M. Catalyst-Counterion Controlled, Regioselective C−C Bond Cleavage in 1-Azabiphenylene: Synthesis of Selectively Substituted Benzoisoquinolines. *ACS Catal.* **2018**, *8*, 10290−10299.
(29) Engelhardt, V.; Garcia, J.-G.; Hubaud, A. A.; Lyssenko, K. A.; Spyroudis, S.; Timofeeva, T. V.; Tongwa, P.; Vollhardt, K. P. C. The Cobalt-Way to Heterophenylenes: Syntheses of 2-Thianorbiphenylenes, Monoazabiphenylenes, and Linear 1-Aza[3]phenylene {Biphenyleno[2,3-*a*]cyclobuta[1,2-*b*]pyridine}. *Synlett* **2011**, 280−284.
(30) Kaupp, M.; Danovich, D.; Shaik, S. Chemistry is about energy and its changes: A critique of bond-length/ bond-strength correlations. *Coord. Chem. Rev.* **2017**, *344*, 355−362.
(31) Zeng, Z.; Jin, H.; Sekine, K.; Rudolph, M.; Rominger, F.; Hashmi, A. S. K. Gold-Catalyzed Regiospecific C−H Annulation of o-Ethynylbiaryls with Anthranils: p-Extension by Ring-Expansion En Route to NDoped PAHs. *Angew. Chem., Int. Ed.* **2018**, *57*, 6935−6939.
(32) Garbe, S.; Krause, M.; Klimpel, A.; Neundorf, I.; Lippmann, P.; Ott, I.; Brünink, D.; Strassert, C. A.; Doltsinis, N. L.; Klein, A. Cyclometalated Pt Complexes of CNC Pincer Ligands: Luminescence and Cytotoxic Evaluation. *Organometallics* **2020**, *39*, 746−756.
(33) Tan, M.-L.; Tong, S.; Hou, S.-K.; You, J.; Wang, M.-X. Copper-Catalyzed N,N-Diarylation of Amides for the Construction of 9,10-Dihydroacridine Structure and Applications in the Synthesis of Diverse Nitrogen-Embedded Polyacenes. *Org. Lett.* **2020**, *22*, 5417−5422.
(34) Luo, C-Z.; Gandeepan, P.; Jayakumar, J.; Parthasararathy, K.; Chang, Y.-W.; Cheng, C.-H. Rh^{III}-Catalyzed CH Activation: A Versatile Route towards Various Polycyclic Pyridinium Salts. *Chem. - Eur. J.* **2013**, *19*, 14181−14186.
(35) Zhao, C.; Ge, Q.; Wang, B.; Xu, X. Comparative investigation of the reactivities between catalysts $[Cp^*RhCl_2]_2$ and $[Cp^*IrCl_2]_2$ in the oxidative annulation of isoquinolones with alkynes: a combined experimental and computational study. *Org. Chem. Front.* **2017**, *4*, 2327−2335.
(36) For similar works, regarding annulations, see Zhou, T.; Li, L.; Li, B.; Song, H.; Wang, B. Syntheses, Structures, and Reactions of Cyclometalated Rhodium, Iridium, and Ruthenium Complexes of N-Methoxy-4-nitrobenzamide. *Organometallics* **2018**, *37*, 476−481.
(37) For definition of PAH's regions see Ozaki, K.; Kawasumi, K.; Shibata, M.; Ito, H.; Itami, K. One-shot K-region-selective annulative π-extension for nanographene synthesis and functionalization. *Nat. Commun.* **2015**, *6*, No. 6251.
(38) Nagamoto, Y.; Yamaoka, Y.; Fujimura, S.; Takemoto, Y.; Takasu, K. Synthesis of Functionalized Polycyclic Aromatic Compounds via a Formal [2 + 2]-Cycloaddition. *Org. Lett.* **2014**, *16*, 1008−1011.
(39) Wu, B.; Yoshikai, N. Conversion of 2-Iodobiaryls into 2,2′-Diiodobiaryls via Oxidation-Iodination Sequences: A Versatile Route to Ladder-Type Heterofluorenes. *Angew. Chem., Int. Ed.* **2015**, *54*, 8736−8739.
(40) McAtee, C. C.; Riehl, P. S.; Schindler, C. S. Polycyclic Aromatic Hydrocarbons via Iron(III)-Catalyzed Carbonyl−Olefin Metathesis. *J. Am. Chem. Soc.* **2017**, *139*, 2960−2963.
(41) Lee, J.; Li, H.; Kalin, A. J.; Yuan, T.; Wang, C.; Olson, T.; Li, H.; Fang, L. Extended Ladder-Type Benzo[k]tetraphene-Derived Oligomers. *Angew. Chem., Int. Ed.* **2017**, *56*, 13727−13731.

https://doi.org/10.1021/acsomega.1c06664
ACS Omega 2022, 7, 8665−8674

(42) Kiel, G. R.; Ziegler, M. S.; Tilley, T. D. Zirconacyclopentadiene-Annulated Polycyclic Aromatic Hydrocarbons. *Angew. Chem., Int. Ed.* **2017**, *56*, 4839−4844.
(43) Donovan, P. M.; Scott, L. T. Diaryl Ketones into Naphthalenes Fused on Two or Four Sides: A Naphthoannulation Procedure. *J. Am. Chem. Soc.* **2004**, *126*, 3108−3112.
(44) Ulč, J.; Nečas, D.; Kotora, M. Unpublished results.
(45) Kawahara, K. P.; Matsuoka, W.; Ito, H.; Itami, K. Synthesis of Nitrogen-Containing Polyaromatics by Aza-Annulative π-Extension of Unfunctionalized Aromatics. *Angew. Chem., Int. Ed.* **2020**, *59*, 6383−6388.
(46) Kong, W.-J.; Shen, Z.; Finger, L. H.; Ackermann, L. Electrochemical Access to Aza-Polycyclic Aromatic Hydrocarbons: Rhoda-Electrocatalyzed Domino Alkyne Annulations. *Angew. Chem., Int. Ed.* **2020**, *59*, 5551−5556.
(47) Fu, W. C.; Wang, Z.; Chan, T. K.; Lin, Z.; Kwong, F. Y. Regioselective Synthesis of Polycyclic and Heptagon-embedded Aromatic Compounds through a Versatile π-Extension of Aryl Halides. *Angew. Chem., Int. Ed.* **2017**, *56*, 7166−7170.

https://doi.org/10.1021/acsomega.1c06664
ACS Omega 2022, 7, 8665−8674